Chapter 3

Modulation of Electronic Relaxation:

Towards Redox-Sensitive Dimeric MRI Agents

Introduction

Chapter 1 of this thesis examined the major factors that contribute to the relaxivity of a gadolinium(III) contrast agent. In that context, the focus was placed upon the relaxivity resulting from inner-sphere water molecules with a cursory acknowledgement of the outer-sphere effects. Briefly, the four main parameters that contribute to the inner-sphere relaxivity are the number of coordinated water molecules, q, the rotational correlation time of the molecule, τ_R, the residence time of the water molecules within the first coordination sphere of the metal ion, τ_m, and the electronic relaxation times, T_e. There are two characteristic electronic relaxation times, the longitudinal time, T_{1e}, and the transverse time, T_{2e}. The β-glucuronidase sensitive contrast agent detailed in Chapter 2 relied upon changes in q to modulate the relaxivity between the unactivated agent and the agent that results upon hydrolysis of the pendant glucuronic acid. Other research has focused on achieving the theoretically optimum τ_m of 1-10 ns and on increasing τ_R, as the small value of this parameter has been implicated as a major impediment to high relaxivity contrast agents.[1, 2]

Very little research has been published on controlling T_e however, presumably because the factors that influence this parameter are not well understood. Merbach and coworkers have shown that Gd(III)-Gd(III) dimer complexes have T_e times that are shorter than monomeric species, but a systematic perturbation of T_e has not been performed. T_e is therefore interesting from both basic and applied science perspectives since the electronic relaxation time is the only parameter that affects both inner- and outer-sphere relaxivity.[1] For activatable contrast agents that are sensitive to external stimuli, the incorporation of T_e modulation permits the development of agents whose

relaxivity in the low relaxivity (unactivated) state, r_{weak}, is negligible. Activatable agents based on modulation of the other parameters mentioned above will always have some residual relaxivity in the unactivated state due to outer-sphere effects. Reduction of r_{weak} to near zero would allow for a larger ratio of relaxivities between the activated and unactivated agents. The higher contrast resulting from this approach is particularly desirable in small molecule gadolinium(III) contrast agents where the relaxivity of the activated agent, r_{strong}, is in the range of 4-8 $mM^{-1}s^{-1}$ with the outer-sphere contributing ~2 $mM^{-1}s^{-1}$ to this value.[1] This chapter discusses a system that is designed to modulate T_e via redox chemistry of a metal ion adjacent to gadolinium(III) through magnetic exchange interactions.

Recall from Chapter 1 that the most effective proton spin relaxation enhancement using a contrast agent will occur when the spectral density function, $J(\omega_H, \tau_c)$, relating the proton Larmor frequency, ω_H, to the contrast agent correlation time, τ_c, is maximal. This occurs when $1/\omega_H = \tau_c$. For inner sphere effects, we have seen that τ_c depends on T_e, τ_m and τ_R. Likewise, outer-sphere effects are governed by T_e and τ_D, the diffusional correlation time that takes into account the bulk water diffusion around the contrast agent.[1] Small molecule gadolinium(III) contrast agents are typically governed by the rotational correlation time τ_R, which is on the order of 0.1 ns, while T_e, the electronic relaxation time for gadolinium(III), is magnetic field dependent and is around 1 ns for the fields employed.[1] Other lanthanides that have larger total angular momentum values due to spin-orbit coupling could be expected to function more effectively than gadolinium(III). This is not the case however because the spin-orbit coupling gives rise to efficient electronic relaxation pathways, resulting in T_e values in the 10^{-13} to 10^{-14}

second range.[3] This makes T_e the dominant factor in τ_c by 3-4 orders of magnitude. The spectral density function is now small at proton Larmor frequencies under study and hence the relaxation gain is minimal even though the magnitude of the dipole is large.

For most MRI experiments the applied magnetic field gives rise to ω_H in the 60-500 MHz range. This means that maximum relaxation enhancement occurs when τ_c is in the 2-20 ns range. Since the reciprocal of τ_c is the sum of the reciprocals of the individual correlation times, (T_e, τ_m and τ_R, for inner-sphere; T_e and τ_D for outer-sphere) the smallest individual correlation time becomes the dominant factor for the total correlation time, τ_c. Thus for the typical small molecule gadolinium(III) contrast agent, τ_R is the shortest correlation time and hence it determines τ_c to a large extent.

If T_e of gadolinium(III) were decreased from 10^{-9} to 10^{-13} to 10^{-14} seconds, τ_c would now be determined by T_e and the resulting contrast agent would have negligible relaxivity. The short T_e compound would function as the unactivated agent, while restoring T_e back to 1 ns would generate the activated agent. To achieve a short T_e for Gd(III), the electrons must be given more relaxation pathways. One way to do this is to exploit magnetic exchange coupling. As discussed in Chapter 1, the magnetic exchange coupling phenomenon arises when the unpaired electrons on two or more paramagnetic metals in close proximity interact through some type of covalent bond. This results in new spin wavefunctions and affects the electronic relaxation times of the metals involved. In the case of two different metals, M_1 (with $T_e = 10^{-13}$ s) and M_2 (with $T_e = 10^{-9}$ s), the electronic relaxation time of M_2 will typically approach that of M_1 even for small J values in the 1-10 cm^{-1} range.[3, 4] This results because M_2 now has additional

relaxation pathways available to it due to the presence of M_1. The small J value required for such an interaction to occur means that even the weak covalent bonds formed by the f-orbitals of the rare earths can result in relaxation enhancement due to exchange coupling.

Placing a paramagnetic metal with a fast T_e, such as Ru(III) ($T_e \sim 10^{-11}$-10^{-12}s) close to Gd(III), should decrease the T_e of Gd(III). This would be the off state of the contrast agent. Reduction of Ru(III) to the diamagnetic Ru(II) would remove the exchange coupling and return the electronic relaxation time of Gd(III) to its normal value. The reduced Ru(II)-Gd(III) compound is then the on state of the agent. Table 3-1 lists a variety of paramagnetic ions along with their T_e's. Perusal of Table 3-1 shows that ruthenium is the best choice for this application since it relaxes quickly as Ru(III) and can readily be reduced to a diamagnetic species, Ru(II); no other ion (except perhaps Fe) possesses these characteristics. The problem now becomes the construction of a ligand system that places the ruthenium and gadolinium ions close enough to each other to allow the manifestation of the magnetic exchange interaction.

The initial target was based on the hexadentate H_2(3,3'-bismethoxy)salen' Schiff base ligand (**1**) shown in Figure 3-1. Here the Ru ion would occupy the N_2O_2 site and the Gd ion would be coordinated in the O_4 site. Costes and coworkers have extensively studied the magnetic interaction between Cu(II) and Gd(III) using this salen' ligand.[5-9] The Cu(II) ion occupies the N_2O_2 pocket while Gd(III) sits in the O_4 coordination site with its coordination sphere completed by nitrate counterions. For the Cu(II)/Gd(III) complexes, the authors have found the exchange interaction to be ferromagnetic with J values ranging from 1.2 to 7.4 cm^{-1}. The magnitude of the interaction appears to depend

Table 3-1: Electronic relaxation times for common metal ions.[3]

Paramagnetic system	**S**	**-log(T_e(s))**
Organic radicals	½	6-8
Ti(III)	½	10-11
VO(II)	½	8
V(III)	1	11
V(II)	3/2	9
Cr(III)	3/2	8.3-9.3
Cr(II)	2	11-12
Mn(III)	2	10-11
Mn(II)	5/2	8
Fe(III) H.S.	5/2	9-11
Fe(III) L.S.	½	11-13
Fe(II) H.S.	2	12-13
Co(II) H.S. 5-6 coord.	3/2	11.3-13
Co(II) H.S. 4 coord.	3/2	11
Co(II) L.S.	½	9-10
Ni(II) 5-6 coord.	1	12
Ni(II) 4 coord.	1	10
Cu(II)	½	9
Ru(III)	½	11-12
Re(III)	2	12-13
Gd(III)	7/2	8-9

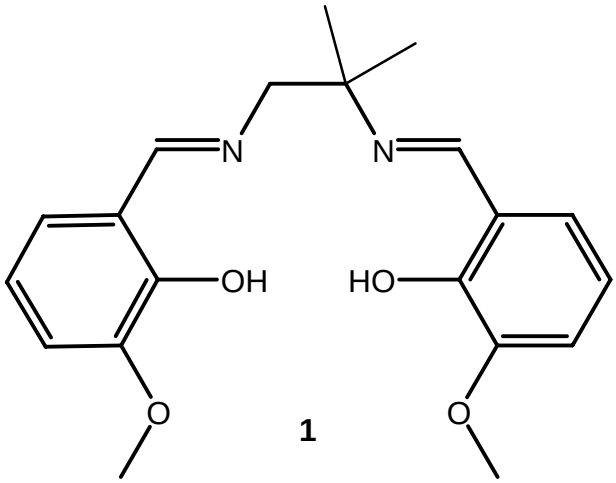

1

Figure 3-1: The hexadentate H_2(3,3'-bismethoxy)salen' Schiff base ligand (**1**).

on the dihedral angle between the two halves (OCuO and OGdO) of the bridging core[5] with any departure from the planar conformation resulting in a weaker interaction. Kahn and coworkers also find the coupling to be dependent on dihedral angle with a J value of 1.4 cm^{-1} observed for a strictly binuclear Cu(II)(salen)(1-methylimidazole) /Gd(III)(hexafluoroacetyacetonato)$_3$ compound having a bridging core dihedral angle of 40°.[10] Neither set of authors makes any relaxation measurements. Since T_e for Cu(II) is comparable to T_e for Gd(III) (Table 3-1), the exchange coupling interaction is expected to have little effect on the relaxivity rate of Gd(III).

Although there is a considerable body of literature for the salen-based 3d / 4f compounds discussed above, the literature on mononuclear Ru(salen) complexes is limited. Much of the older Ru(salen) literature deals with the use of the complex as a catalyst for organic oxidations[11] and details the reversible O_2 and CO binding properties of the complex.[12-14] The lack of literature appears to stem from the fact that the Ru(III)(salen) system is not a very good catalyst compared to others such as Mn(III)(salen) complexes.[11] Recently, however, there has been more interest in Ru(II)(salen)(NO) complexes. These complexes have been shown to be precursors for oxene and carbene transfer catalysts.[15-18] Irradiation photolabilizes the NO ligand resulting in oxidation to Ru(III) and the opening of a coordination site on the metal center. The product appears to be a solvento species based on the solvent dependent rate of the back reaction with NO.[19]

Results and Discussion

Ru(III)(3,3'-bismethoxy)salen' compounds: Synthesis and characterization

The initial route to the Ru(III)/Gd(III) dyad consisted of synthesis of the Ru(III) salen' compounds (Scheme 3-1) followed by metallation with a Gd(III) salt. This route is based on the closely related synthesis of the underivatized Ru(III)salen analog.[11] Condensation of two equivalents of 3-methoxysalicylaldehyde with one equivalent of 1,2-diamino-2-methylpropane in MeOH generated salen' ligand **1**. The ligand was recrystallized from hot toluene in 89% yield. Formation of the Ru(III)(3,3'-bismethoxy)salen'(PPh_3)Cl compound **2** was achieved via aerobic oxidation of Ru(II)(PPh_3)$_3$$Cl_2$ in the presence of **1**. This reaction is based on the analogous reaction to form Ru(III)(salen)(PPh_3)Cl.[20] The purification of **2** from other oxidized species was not trivial and required a two-step process wherein the crude product was precipitated from THF using hexanes and subsequently recrystallized from THF. The recrystallized compound was green in color and turned brown upon washing with diethyl ether, indicating the lability of the chloride ligand. Presumably the compound is a THF adduct initially and washing with ether converts the solvento species into the chloride compound. This generated analytically pure **2** in low yield. Subsequent studies indicated that initial formation of the Ru(II)salen' species followed by aerobic oxidation generated **2** in higher yield by avoiding intermediate oxidation processes.

Conversion of **2** into the biscyano species **3** was accomplished using two equivalents of sodium cyanide in methanol. The compound was recrystallized from hot EtOH. The use of exactly two equivalents of cyanide alleviated any problems associated with removal of excess sodium cyanide. The cyanide ligand was chosen as the axial ligand for ruthenium because of the strong bond it would form with the metal center and its ability to render the resulting compound water soluble. The aqueous solubility of the

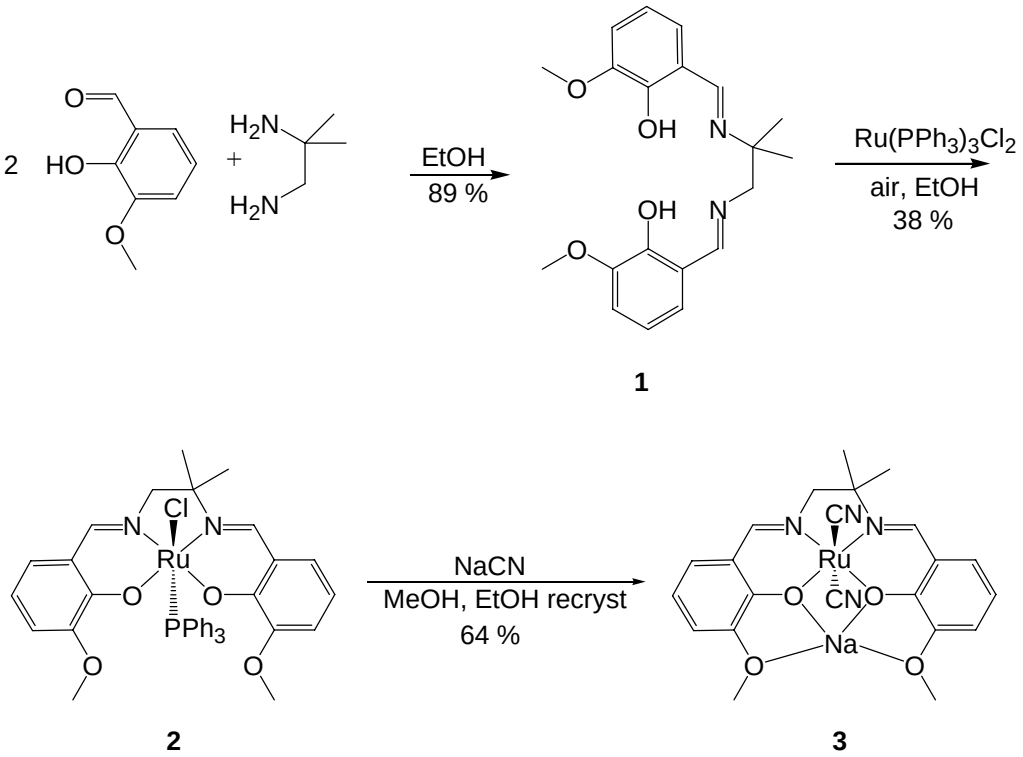

Scheme 3-1: Synthesis of Ru(III)(3,3'-bismethoxy)salen' compounds.

final dyad is essential if the complex is to function as an MRI contrast agent in water.

It was initially anticipated that the cyanide ligands would generate a compound whose Ru(II)/Ru(III) couple would be more positive than the couple of molecular oxygen allowing both states to be air-stable. Measurement of the redox potential of **3** in water however gave an $E_{1/2}$ of -357 mV vs Ag/AgCl indicating that the Ru(II) compound is air-sensitive. This is reasonable as the monoanionic charge of each cyanide ligand shifts the potential more negative, more than compensating for the π acidity of the ligand.

The electrochemistry of **3** showed quasi-reversibility at a scan rate of 100 mV / s. The peak separation, ΔE_p, between the anodic and cathodic waves was 115 mV, far from the 59 mV standard for reversibility, and the ratio of peak currents, i_{pc}/i_{pa}, was equal to 1.15 instead of unity. Comparison with the electrochemistry of the structurally similar Na[Ru(salen)$(CN)_2$], which displayed a reversible couple at $E_{1/2}$ = -315 mV (vs Ag/AgCl), indicates that the quasi-reversibility of **3** may be due to a coordination equilibrium involving the sodium counterion. The sodium ion can be coordinated by the O_4 site comprised of the two phenolic oxygens and the two methoxy groups on ligand **1** when the compound is in the Ru(III) state (see the crystallography section below). The reduced Ru(II) compound is neutral and thus the sodium counterion is no longer required. In the Na[Ru(salen)$(CN)_2$] case there are no coordination sites for sodium so the redox chemistry is not associated with a counterion coordination equilibrium.

Ru(III)(3,3'-bismethoxy)salen' compounds: X-ray crystallography

Single crystals of compound **2** were obtained from diffusion of diethyl ether into an acetone solution of the compound. A view of the solved structure is given in Figure 3-

2. The Ru(III) center sits in an octahedral site with a P1-Ru1-Cl1 angle of 172.48(5)°. The crystallographic details for **2** along with the metrics for **3** are listed in Table 3-2 with selected bond lengths and angles given in Table 3-3. X-ray quality crystals of **3** were grown from slow cooling of a hot saturated methanolic solution of the compound. Comparison of **2** with the structure of **3** shows the subtle differences in geometry around the Ru(III) center that result from changing the axial ligands. In **3**, the sodium counterion is chelated in the O_4 site, the same position designed for gadolinium(III) occupation. The Na1-O1-O2-Ru1 torsion angle is 175.82°, which is a deviation from planarity of 4.18°. Maintaining such a small distortion from planarity upon substitution of Gd(III) for Na(I) would allow nearly maximal magnetic interaction between Ru(III) and Gd(III) via the oxo bridges.

Reaction of Gd(III) with Ru(III)(3,3'-bismethoxy)salen' compounds

With water soluble compound **3** in hand the coordination chemistry with gadolinium(III) was explored. Initially, **3** was suspended in acetonitrile and a slight excess of Gd(III)$(NO_3)_3$ dissolved in acetonitrile was added. This gave a blue solid that was soluble in methanol. Layering of diethyl ether onto a methanolic solution of the blue solid generated a small amount of X-ray quality crystals after two months. These crystals did not diffract well (the refined structure had a weighted R_2 of 0.3426) and the structure was entirely unexpected (Figure 3-4)! Instead of having a Gd(III) ion sitting in the O_4 site of the salen-based ligand, the complexes dimerized with loss of a cyanide ligand. The dimers further assembled into a trimer of dimers motif via sodium counterions that bridged between dimers through the aryl methoxy groups. Based on the ligands and

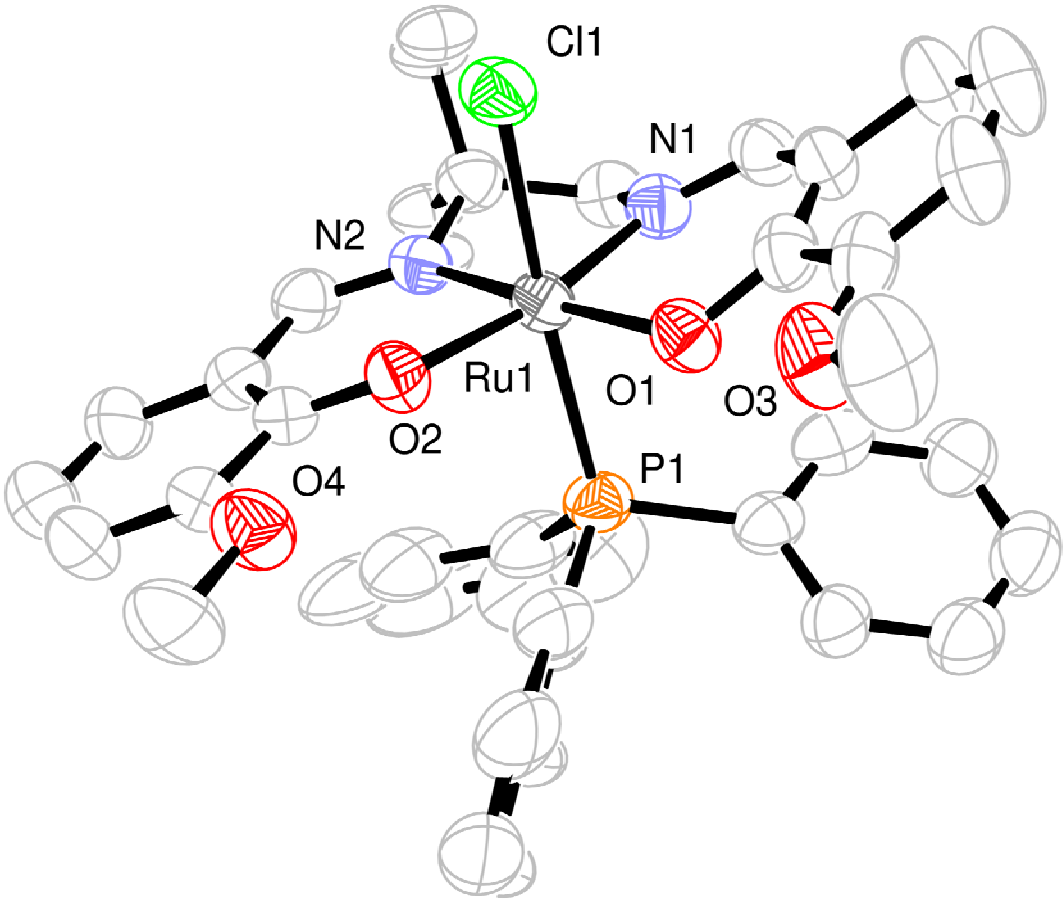

Figure 3-2: Thermal ellipsoid (50%) depiction of compound **2**. The acetone solvate and hydrogen atoms have been removed for clarity. The methyl groups on the ethylenediamine backbone show some disorder.

Table 3-2: Crystallographic details for **2** and **3**.

	2•1/4acetone	**3**•3/2MeOH
Empirical formula	$C_{38.75}H_{37}ClN_2O_{4.25}Ru$	$C_{23.5}H_{26.5}N_4NaO_{5.5}Ru$
Formula weight	766.19	577.05
Crystal system	Monoclinic	Monoclinic
Space group	*C2/c*	$P2_1/n$
a (Å)	41.529(11)	13.352(4)
b (Å)	13.435(3)	9.595(3)
c (Å)	13.293(4)	20.994(7)
β (°)	92.10(3)	98.822(5)
V (Å^3)	7412(3)	1878.3(4)
Z	8	4
ρ (calc) (g cm^{-3})	1.374	1.442
μ (mm^{-1})	0.580	0.647
Reflections collected/unique	34095/9058 [R_{int} = 0.0695]	24118/6517 [R_{int} = 0.0554]
Data/restraints/parameters	9058/0/446	6517/0/331
Goodness-of-fit on F^2	0.961	1.076
Final *R* indices [$I>2(\sigma)I$]	R_1 = 0.0549, wR_2 = 0.1478	R_1 = 0.0530, wR_2 = 0.1472
R indices (all data)	R_1 = 0.1316, wR_2 = 0.1928	R_1 = 0.0717, wR_2 = 0.1617

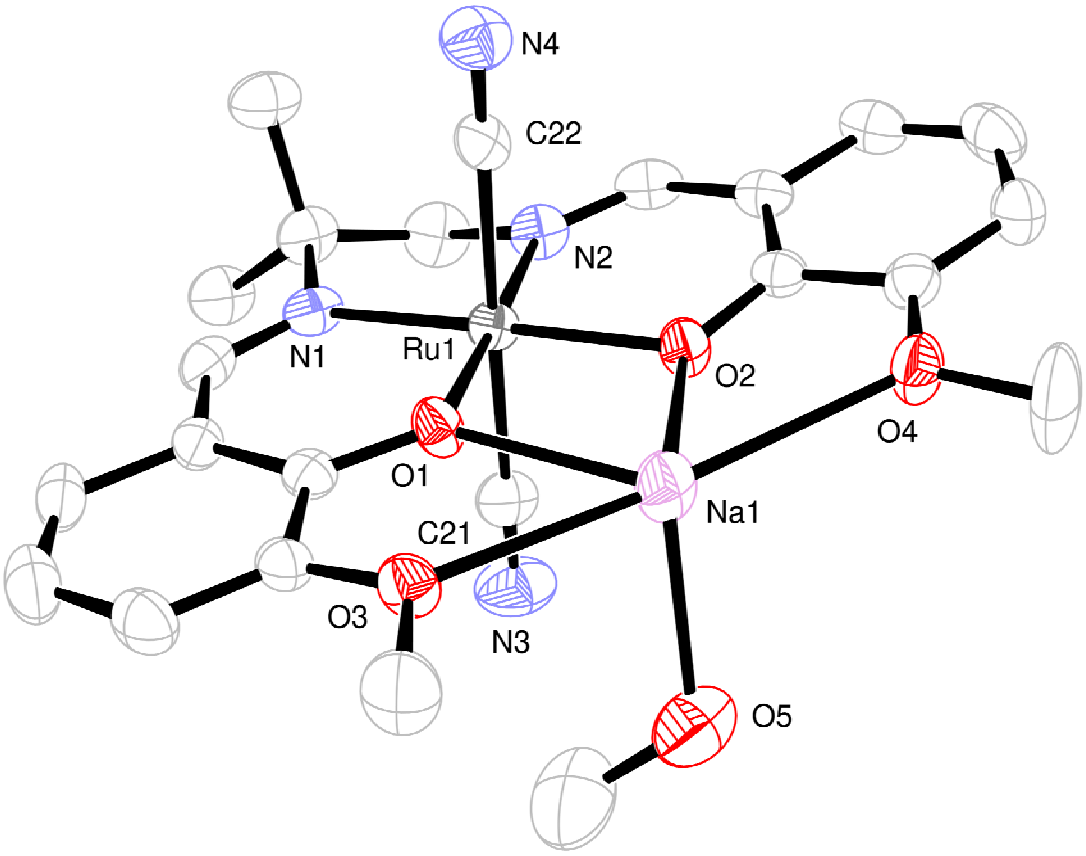

Figure 3-3: Thermal ellipsoid (50%) depiction of **3**. A half-occupancy, uncoordinated methanol solvate and all hydrogen atoms have been removed for clarity.

Table 3-3: Selected bond lengths (Å) and angles (°) for compounds **2** and **3**.

	2•1/4acetone	**3**•11/2MeOH
Ru(1)-N(1)	1.973(4)	1.983(3)
Ru(1)-O(1)	1.990(3)	2.006(3)
Ru(1)-N(2)	2.009(4)	1.969(3)
Ru(1)-O(2)	2.024(3)	1.998(3)
Ru(1)-P(1)	2.3468(14)	--
Ru(1)-Cl(1)	2.4370(14)	--
Ru(1)-C(21)	--	2.079(5)
Ru(1)-C(22)	--	2.093(4)
Ru(1)-Na(1)	--	3.3935(18)
C(21)-N(3)	--	1.147(6)
C(22)-N(4)	--	1.148(6)
C(21)-Ru(1)-C(22)	--	178.70(15)
P(1)-Ru(1)-Cl(1)	172.48(5)	--
N(3)-C(21)-Ru(1)	--	177.1(4)
N(4)-C(22)-Ru(1)	--	177.1(4)
Na(1)-O(1)-O(2)-Ru(1)	--	175.82

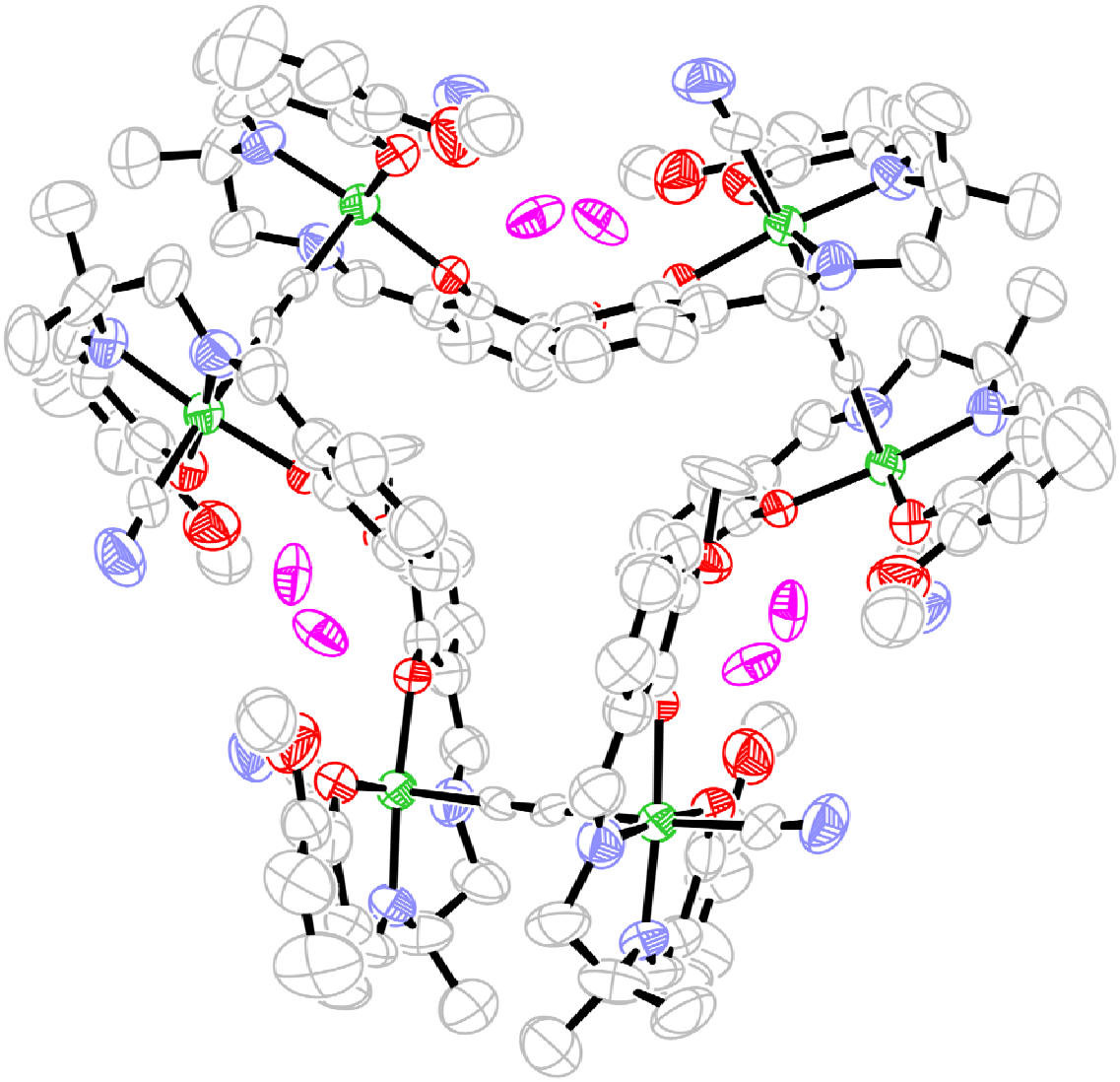

Figure 3-4: Thermal ellipsoid (50%) of the Ru(III)-Ru(III) trimer of dimers, **4**. Ru atoms are green, N atoms are blue, O atoms are red and Na atoms are magenta. The compound crystallized in a cubic space group and hence the asymmetric unit is one half of one dimer. Thus the sodium atoms are depicted at half-occupancy and the bridging cyanide is shown as two undefined atoms. For clarity, all bonds to the sodium atoms have been removed as have the methanol molecule and water molecule coordinated to each sodium atom. A cocrystallized water molecule has also been omitted.

Table 3-4: Crystallographic details for **4** and **5**.

	4	**5**
Empirical formula	$C_{21.5}H_{22}N_{3.5}Na_{0.5}O_{4.75}Ru$	$C_{84}H_{94}N_4O_{27}GdP_2Ru_2$
Formula weight	517.99	2013.02
Crystal system	Cubic	Triclinic
Space group	*Fd-3c*	$P\bar{1}$
a (Å)	51.366(4)	13.514(9)
b (Å)	51.366(4)	13.733(7)
c (Å)	51.366(4)	26.358(16)
α (°)	90	87.22(5)
β (°)	90	85.44(7)
γ (°)	90	63.14(5)
V (Å^3)	135521(19)	4350(4)
Z	192	2
ρ (calc) (g cm^{-3})	1.219	1.537
μ (mm^{-1})	0.592	2.015
Reflections collected/unique	299965/7409 [R_{int} = 0.3205]	12339/4952 [R_{int} = 0.2390]
Data/restraints/parameters	7409/0/302	4952/0/701
Goodness-of-fit on F^2	1.091	0.862
Final *R* indices [$I>2(\sigma)I$]	R_1 = 0.1407, wR_2 = 0.3426	R_1 = 0.0900, wR_2 = 0.2037
R indices (all data)	R_1 = 0.3024, wR_2 = 0.4121	R_1 = 0.2039, wR_2 = 0.2548

counterions it was determined that all ruthenium ions were Ru(III). Crystallographic data for the dimer structure, **4**, are listed in Table 3-4.

Although the structure did not contain gadolinium ions, ICP-MS analysis of the initial blue solid formed in the reaction confirmed that gadolinium was present in the solid at a 2:3 Ru:Gd ratio. The crystals of the blue solid were obtained only after the crystal growth experiment was allowed to sit for an extended period. Given the long time period required for crystallization, it is conceivable that the compound that crystallized was either not indicative of the bulk material or that it reflected a product formed over the course of the crystallization experiment.

The lack of structural evidence for gadolinium(III) chelation by the O_4 site of the salen-based ligand indicated that even if Gd(III) were chelated the binding constant could be low. Thus the ion may not stay coordinated in aqueous solution. For the Ru-Gd dyad magnetic properties to be examined, Gd(III) must be at least 99.9% coordinated. This percentage translates into a binding constant of roughly 10^3. The binding of the tri-positive Gd(III)cation to the (3,3'-bismethoxy)salen' ligand should reduce the electron density at the Ru(III) center, resulting in a change in the absorption spectrum of the compound. To test this possibility, the absorption spectrum of a 0.2 mM solution of compound **3** in water was recorded and compared with the spectrum resulting from addition of five equivalents of $Gd(III)(NO_3)_3$. The spectra showed no difference. The results were the same using $Gd(III)Cl_3$. Similar experiments in methanol and DMF also showed no change upon addition of Gd(III). The use of the tetra-*n*-butyl ammonium salt of **3** instead of the sodium salt had no effect on the spectra. Based on these observations, compound **3** does not chelate Gd(III) well.

With the knowledge that **3** functioned poorly for the Ru-Gd dyad, the non-aqueous soluble **2** was examined for solid state binding of Gd(III). While the Ru-Gd dyad resulting from **2** would presumably be insoluble in water, the magnetic susceptibility of a solid state compound could be a proof of principle for the Ru-Gd magnetic interaction. To test this, compound **2** was dissolved in acetone and 1.2 equivalents of $Gd(III)(NO_3)_3$ were added. The red-brown solid formed upon cooling was recrystallized at 4 °C by vapor diffusion of diethyl ether into acetonitrile. The resulting X-ray quality crystals revealed the structure shown in Figure 3-5, with the crystallographic metrics summarized in Table 3-4. The diffraction data for this crystal was poor but connectivity could be established. Here, Gd(III) is included in the structure but functions as a counterion rather than becoming part of a Ru-Gd dyad. The $Gd(III)(NO_3)_5^{2-}$ anion balances two Ru(III) complexes that contain an axial triphenyl phosphine and an axial water molecule. This result indicates that the nitrate anion functions as a better ligand than the salen-based ligand for Gd(III). Attempts to grow crystals using other Gd(III) salts such as the triflate or the chloride were unsuccessful.

Consideration of the above data leads to the conclusion that the (3,3'-bismethoxy)salen' ligand is not viable for formation of a solution stable Ru-Gd dimer. The next section discusses progress toward a better ligand that substitutes the anionic carboxylate group for the methoxy substituent.

Bis-carboxylate salen ligands: Synthesis

To overcome the Gd(III) chelation difficulties encountered using the (3,3'-bismethoxy)salen' ligand, ligands containing carboxylate groups instead of methoxy

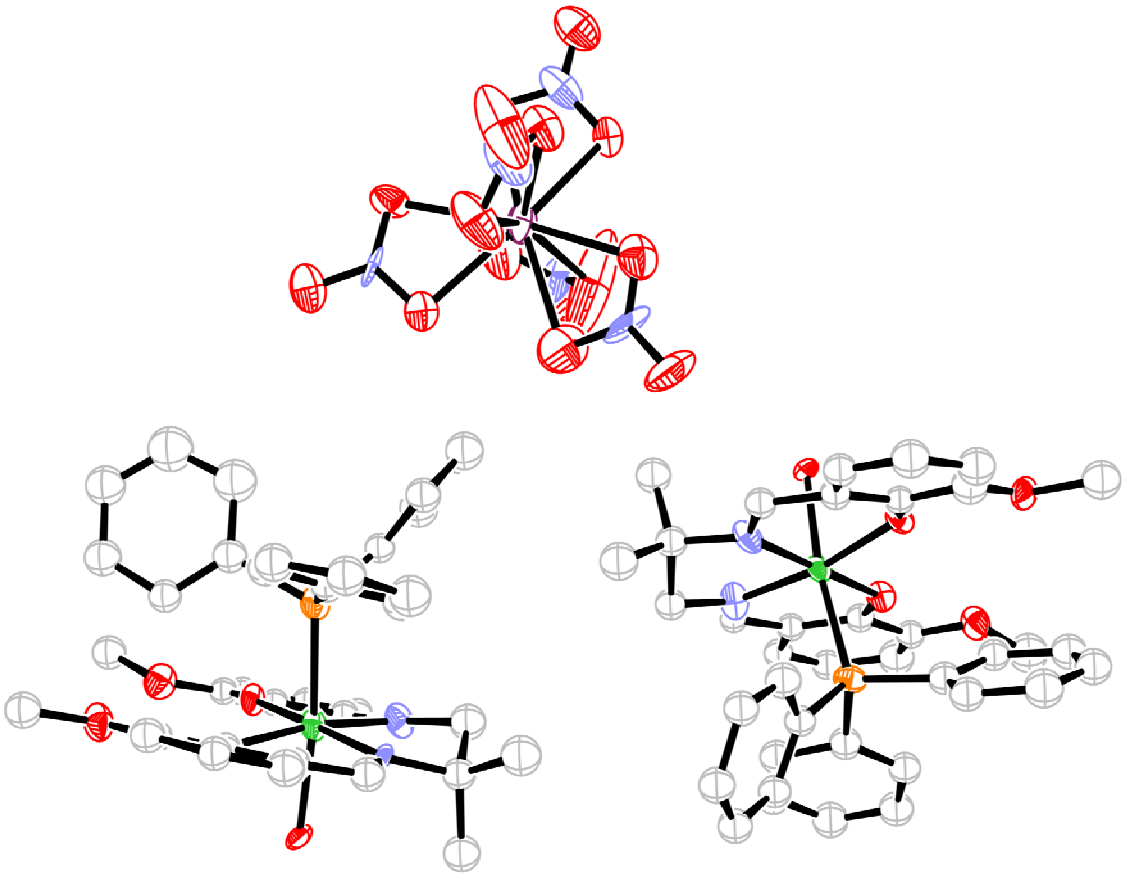

Figure 3-5: Thermal ellipsoid (50%) depiction of **5**. Ru atoms are green, P atoms are orange, O atoms are red, N atoms are blue and Gd atoms are purple. Two diethyl ether molecules have been removed for clarity.

groups were investigated. The general structure of this class of ligand is displayed in Figure 3-6. The negative charge and smaller pocket of the carboxylate containing ligand were anticipated to provide better chelation of Gd(III). Many dinuclear compounds based on the ligands in Figure 3-6 containing a 3d ion in the N_2O_2 site and a lanthanide in the O_4 site have been made and magnetically and structurally characterized by the Sakamoto group.[21-26] The magnetic data typically shows an exchange interaction between the 3d and 4f ions on the order of 1-10 cm^{-1}. Most of these reports focus on solid state measurements; the solution properties of these compounds have rarely been examined. The studies have been confined to 3d ions that lack strongly bound axial ligands and no reports have been published on ruthenium containing dyads.

Three main approaches were pursued in the synthesis of (3,3'-biscarboxy)salen ligands. The first is the Duff reaction where salicylic acid is formylated using hexamethylenetetraamine followed by hydrolysis (Figure 3-7).[27, 28] This reaction generates both the *ortho*- and *para*-formylation products which are difficult to separate. Jacobsen and coworkers have optimized yields for production of several formylated salicylic acids by carefully controlling the temperature and time of the reactions.[29] These compounds contain *tert*-butyl groups and are designed to be soluble in organic solvents. Synthesis of 3-formyl salicylic acid via this approach always yielded product that was contaminated with the *para*-isomer, 5-formyl salicylic acid.

An alternative route to 3-formyl salicylic acid using photobromination was then investigated. In this literature procedure the methyl group in 3-methyl salicylic acid is dibrominated and then hydrolyzed to give the aldehyde.[30] The procedure did not work well due to the fact that the monobrominated compound was insoluble in the reaction

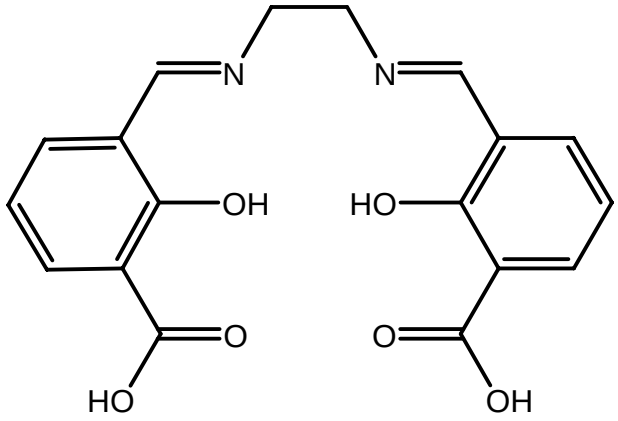

Figure 3-6: General structure of (3,3'-biscarboxy)salen ligands.

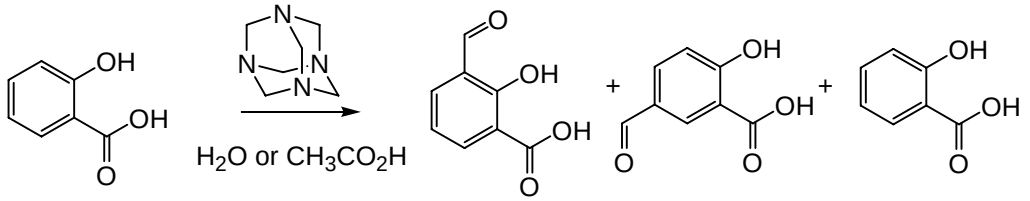

Duff Reaction

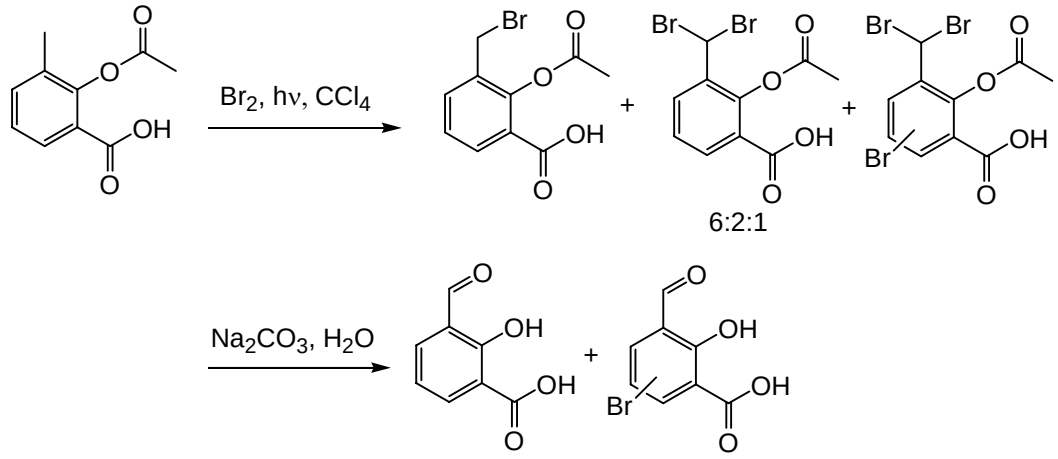

Photobromination

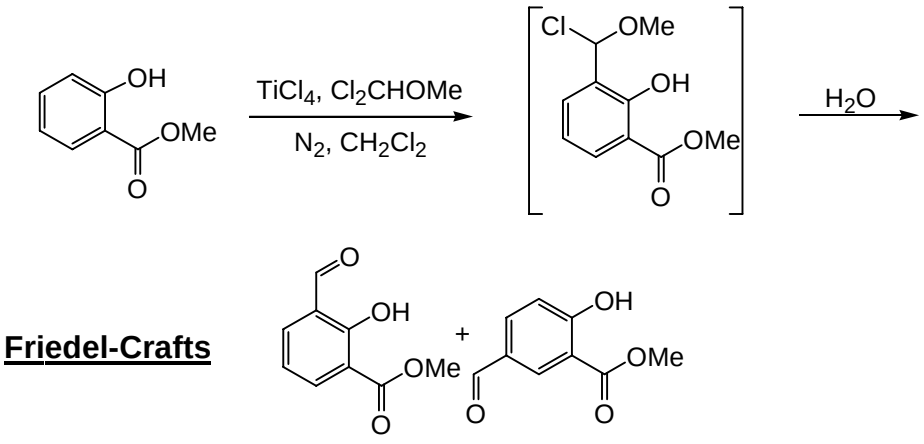

Friedel-Crafts

Figure 3-7: Three synthetic approaches to 3-formyl salicylic acid.

solvent and hence the reaction stopped at monobromination. Changing the solvent to allow the monobromide to be soluble resulted in many side products where the aryl ring was also brominated. The yield of the desired compound was quite low and this approach was not pursued further.

The best synthesis of 3-formyl salicylic acid involved the formation of 3-formyl methyl salicylate, a compound that proved to be more useful than the free acid due to its increased solubility in organic solvents (Scheme 3-2). The key step in this procedure was a $TiCl_4$-catalyzed Friedel-Crafts alkylation of methyl salicylate using Cl_2CHOMe.[31] This reaction also gives a mixture of products substituted *ortho*- and *para*- to the hydroxyl position but favors *ortho* substitution due to Ti coordination to the hydroxyl. The yield for this route was not optimized but enough material was produced for subsequent studies. The 4-methyl derivative could also be formed using this approach. Formation of (3,3'-bismethyloxycarbonyl)salen, **6**, and (3,3'-bismethyloxycarbonyl-4,4'-dimethyl)salen, **7**, were achieved through condensation with ethylenediamine in EtOH.

Bis-carboxylate salen ligands: Reaction with ruthenium

Several metallation reactions of organic soluble compounds **6** and **7** were investigated using various ruthenium starting materials. Initial attempts focused on the Ru(III) salt, $K_2RuCl_5(H_2O)$. Reactions using this paramagnetic compound were quite difficult to characterize and follow; thus the chemistry of $Ru(II)(DMSO)_4Cl_2$[32] was pursued. Use of this diamagnetic Ru(II) material allowed for characterization through ^1H NMR spectroscopy but required air-free conditions to prevent oxidation to Ru(III). Reaction of **6**, $Ru(II)(DMSO)_4Cl_2$ and various bases, including substituted pyridines for

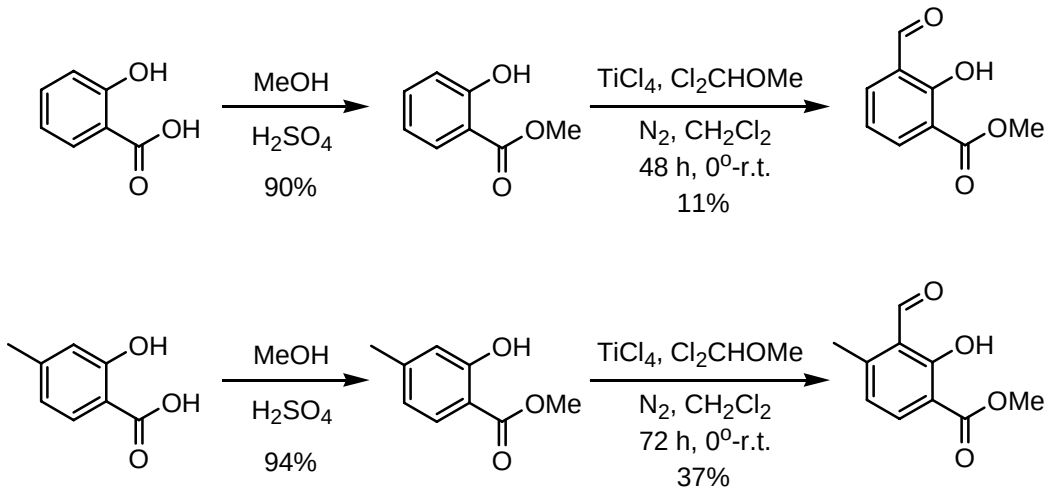

Scheme 3-2: Synthesis of 3-formyl methyl salicylate and 3-formyl-4-methyl methyl salicylate via $TiCl_4$-catalyzed addition of Cl_2CHOMe.

axial ligands, indicated that the Ru(II) ion was coordinated by the ligand but that the ligand underwent decomposition. Mass spectral and NMR data showed that the diimine backbone hydrolyzed during the reaction generating the coordinated salicylic acid and free ethylenediamine. Presumably the electron withdrawing methyl ester polarizes the imine making it more susceptible to hydrolysis. While exclusion of water should prevent this decomposition, the water sensitivity of the compound makes the subsequent ester hydrolysis and Gd(III) chelation steps difficult. Furthermore the Ru-Gd dyad should function in water and therefore should be water stable. The solution to this problem lies in making a ligand without the sensitive imines.

Towards robust dinucleating phenanthroline based ligands

Replacement of the ethylenediamine backbone with an inert phenanthroline core circumvents the potential hydrolysis of the polarized imine bonds in the (3,3'-bismethyloxycarbonyl)salen ligands discussed in the previous section. This makes the ligand synthesis more involved but several analogs that retain the N_2O_2 core and contain pyridyl or phosphine donors have been synthesized (Figure 3-8).[33] The proposed route to a phenanthroline containing carboxylate functionalized ligand is shown in Scheme 3-3. The initial steps toward the desired ligand have been accomplished.

Radical bromination using NBS in the presence of diisopropyl amine gave the bromo phenol **10** in high yield.[34] Methylation with dimethyl sulfate generates **9** in 89% yield. Lithium / halogen exchange of **9** yields the aryl anion, which was reacted with 1,10-phenanthroline to generate intermediate **11** in poor yield (9.6%). The aryl-aryl coupling is an initial result and the reaction needs to be explored more fully. The initial

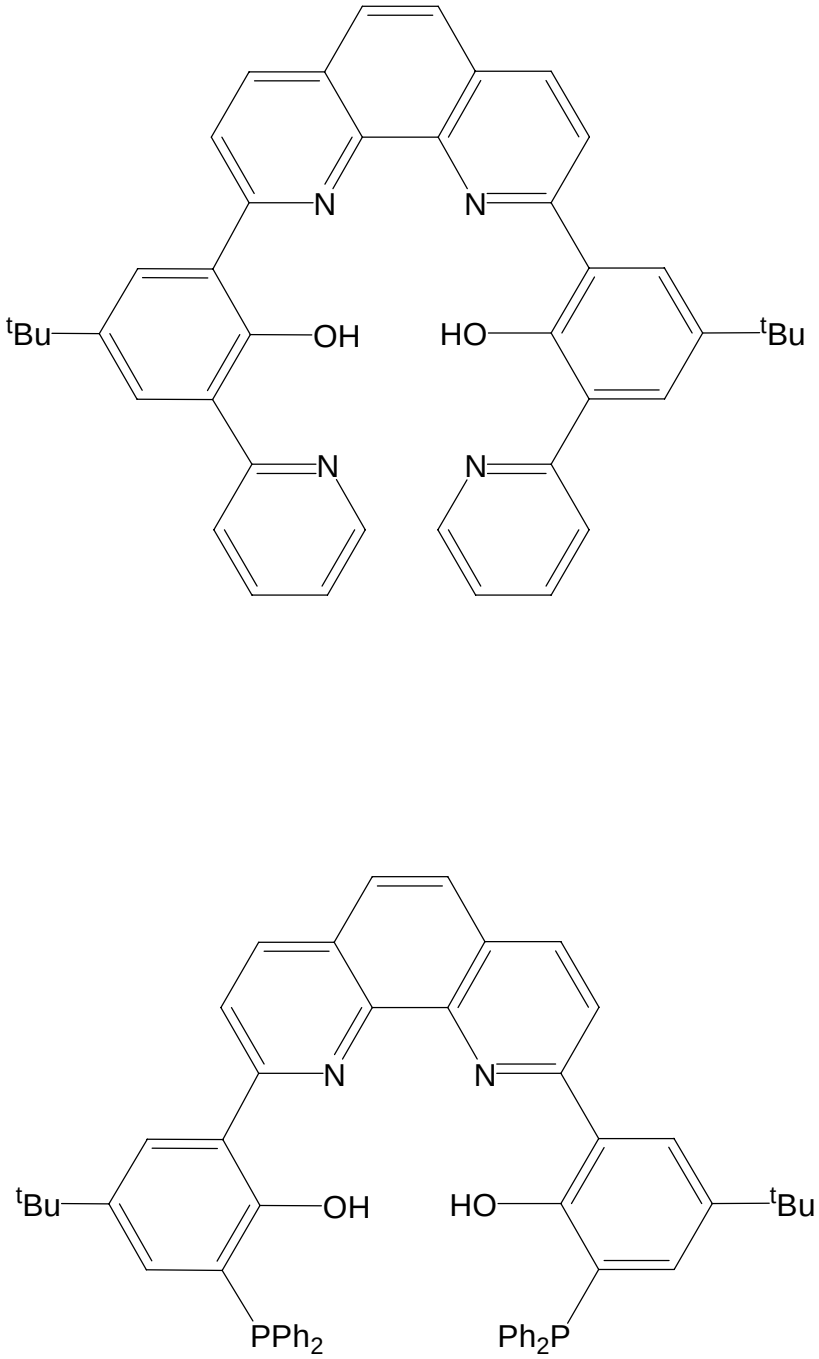

Figure 3-8: Phenanthroline-based dinucleating ligands.

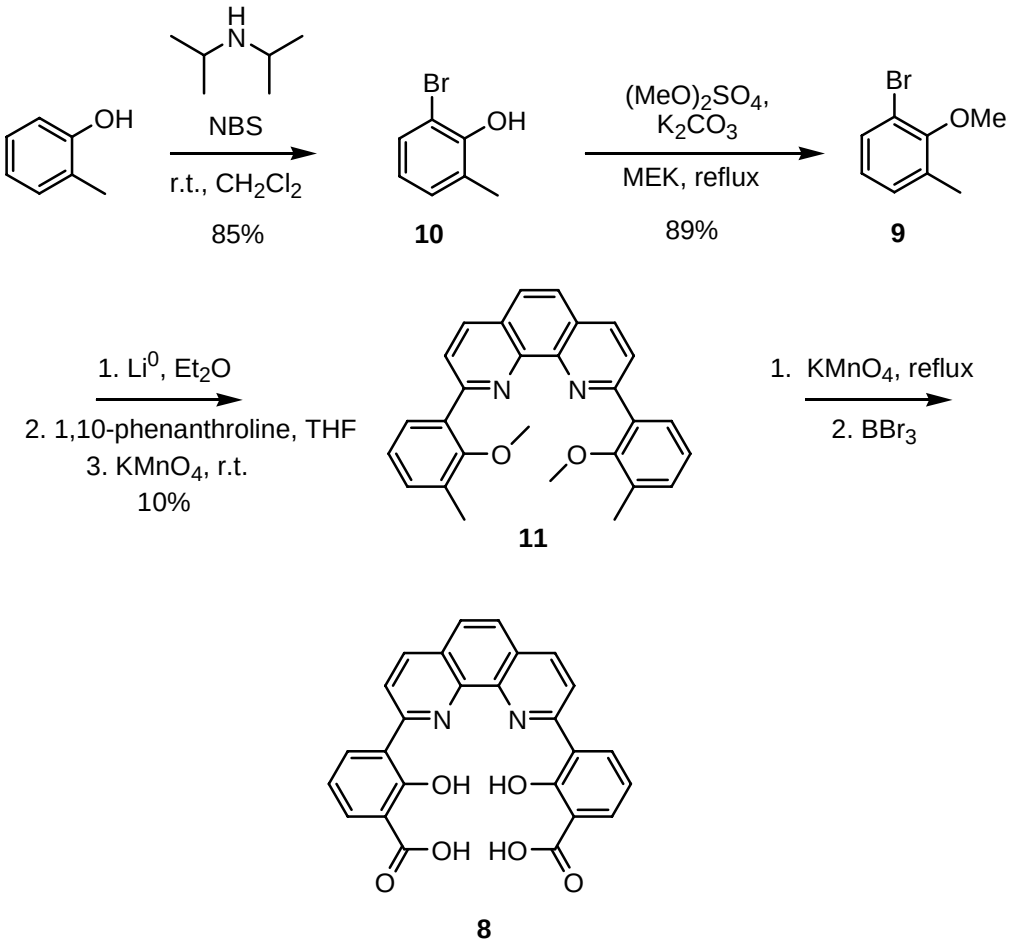

Scheme 3-3: Progress toward a dinuclear chelating phenanthroline ligand, **8**.

results for Scheme 3-3 look promising and should lead to a more robust ligand for the Ru-Gd dyad. The water solubility of the complex can be adjusted using carboxylate derivatized axial pyridyl ligands on the ruthenium center. The structure shown in Figure 3-9 depicts the target molecule.

Conclusion and Further Studies

Control of the relaxivity of Gd(III)-based magnetic resonance imaging contrast agents via modulation of q, the number of inner-sphere water molecules coordinated to the metal center, and τ_R, the rotational correlation time of the agent, has been examined by many researchers. Using the electronic relaxation times, T_e, to vary the relaxivity has not been demonstrated. This chapter detailed work towards Ru-Gd dyads designed to modulate T_e of Gd(III) via the redox state of the ruthenium center. Ru(III) has a short T_e and thus should accelerate the electronic relaxation of Gd(III), generating a contrast agent of negligible relaxivity. One electron reduction of Ru(III) generates diamagnetic Ru(II), which does not magnetically couple to Gd(III), thus generating the high relaxivity agent.

The original system proposed for the Ru-Gd dyad consisted of a (3,3'-bismethoxy)salen' ligand. While the Ru(III) compounds of this ligand were synthesized and structurally characterized, attempts to coordinate Gd(III) in the O_4 coordination site comprised of two phenolic oxygen atoms and two methoxy groups were unsuccessful. Instead, the isolated compounds contained the structurally characterized Ru(III) dimer, **4** and the monocationic Ru(III)(3,3'-bismethoxy)salen'(PPh_3)(H_2O) compound balanced by one half of one equivalent of Gd(III)$(NO_3)_5^{2-}$ (Figure 3-5). These results combined with

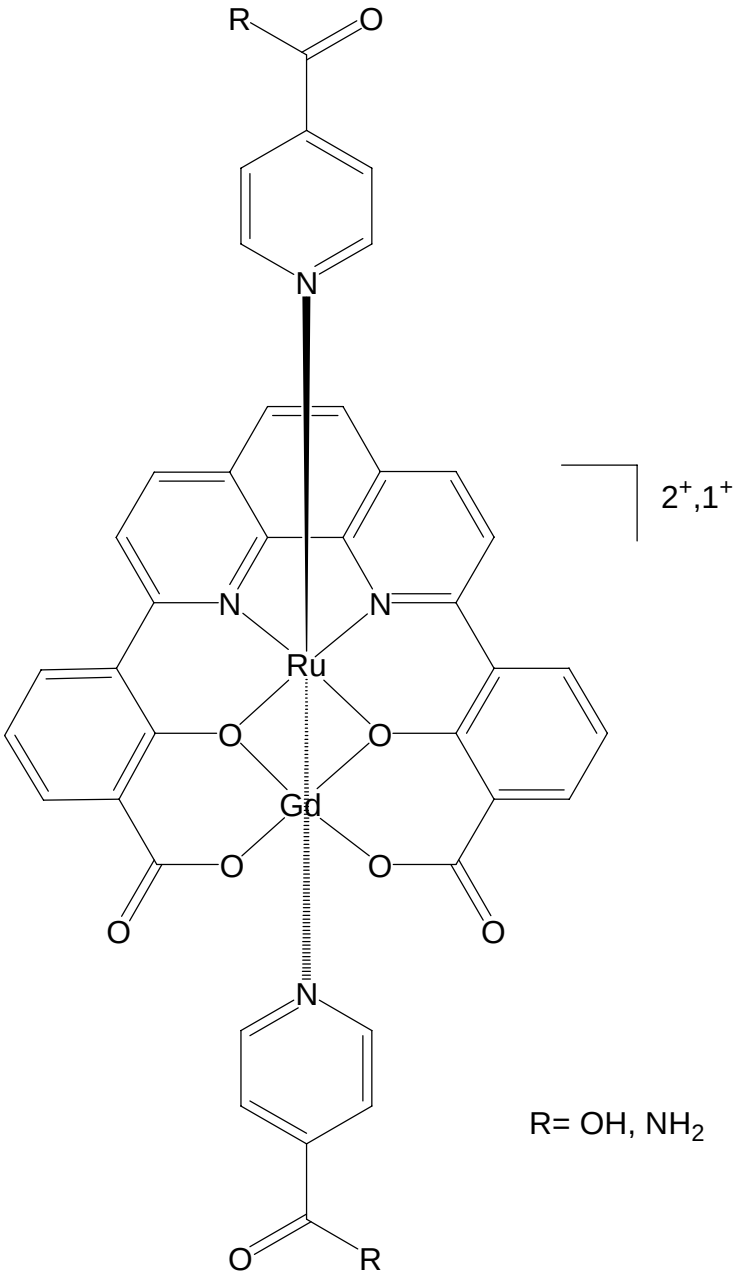

Figure 3-9: Proposed Ru-Gd dyad using the phenanthroline-based ligand **8**. When Ru is tripositive the overall charge is 2+, when Ru is dipositive the overall charge is 1+.

aqueous Gd(III) binding studies indicated that a (3,3'-bismethoxy)salen' would not effectively coordinate gadolinium(III).

Carboxylate groups were introduced into the salen-based ligand to increase the binding affinity for Gd(III). The introduction of the electron-withdrawing carboxylates polarized the imine backbone in the ligand, increasing the susceptibility for hydrolysis. Thus, attention was directed to a phenanthroline derived ligand that should not be susceptible to hydrolysis. Initial work towards this ligand set indicated that the approach is viable and should be pursued.

Once the Ru-Gd dyad has been made, the relaxivity of the compound as a function of ruthenium oxidation state should be measured. These results can be compared with temperature dependent magnetic susceptibility data to analyze the effect the ruthenium center has on the Gd(III) electronic relaxation rates. With this knowledge in hand the dyad may be tested in vitro for toxicity and the agent could be used as a redox sensitive MRI probe.

Experimental

General Methods:

Unless otherwise mentioned, all reagents were used as purchased. $Ru(PPh_3)_3Cl_2$ was obtained from Strem. $Ru(DMSO)_4Cl_2$ was prepared by the literature method.[32] Dry solvents where indicated were dried via an activated alumina drying system. NMR spectra were recorded on either a Varian Mercury 400 MHz or Varian Inova 500 MHz instrument. Peaks were referenced to an internal TMS standard. Electrospray mass spectra were obtained via direct infusion of a methanolic solution of the compound of

interest on a Varian 1200L single quadrupole mass spectrometer. Elemental analysis was performed by Desert Analytics (Tucson, AZ). ICP-MS were recorded on a VG Elemental PQ Excell spectrometer standardized with eight concentrations spanning the range 0-50 ppb Gd(III) and Ru(III). One ppb In(III) was used as the internal standard for all runs. Electrochemical studies were performed in N_2 sparged, 100mM NaCl aqueous solutions using a standard three electrode configuration consisting of a glassy carbon working electrode, a platinium wire counter electrode and a Ag/AgCl reference electrode. The measurements were made on a CH Instruments 660A workstation. UV-visible spectroscopy was performed on a HP 8452A diode array spectrometer at room temperature.

(3,3'-bismethoxy)salen': (1)

To a solution of *o*-vanillin (2.00 g, 13.1 mmol) in MeOH (15 mL) at room temperature was added a solution of 1,2-diamino-2-methylpropane (692 μL, 6.6 mmol) in MeOH (10 mL) over 5 min. The yellow solution was refluxed for 1 h and the solvent removed *in vacuo*. The crude product was recrystallized from hot toluene to afford 2.09 g (89%) **1**. ^{1}H NMR (400 MHz, $CDCl_3$): δ 1.43 (s, 6H), 3.72 (s, 2H) 3.88 (s, 6H), 6.75-6.79 (m, 2H), 6.84-6.90 (m, 4H), 8.29 (m, 2H); ^{13}C NMR (100 MHz, $CDCl_3$) δ 25.4, 56.2, 60.3, 70.2, 113.8, 113.9, 117.7, 118.0, 118.3, 118.4, 123.1, 123.3, 148.2, 148.4, 151.6, 152.3, 161.6, 166.6; Anal. Calcd for $C_{20}H_{24}N_2O_4$: C 67.40, H 6.79, N 7.86. Found: C 67.49, H 6.70, N 7.69.

Ru(III)(3,3'-bismethoxy)salen'(PPh_3)Cl: (2)

Triethylamine (2.94 mL, 21.1 mmol), Ru(II)$(PPh_3)_3Cl_2$ (5.05 g, 5.27 mmol) and **1** (1.88 g, 5.27 mmol) were combined in EtOH (125 mL). The solution was refluxed and

air was allowed to bubble through for 20 h at which point the mixture was filtered through Celite and the solvent removed *in vacuo*. The crude green material was dissolved in THF (60 mL) and precipitated upon addition of hexanes (350 mL). The precipitate was washed with hexanes (3 x 20 mL) and recrystallized from hot THF yielding 1.50 g (38%) of **2**. X-ray quality crystals were obtained upon 2 x vapor diffusion of diethyl ether into acetone. ESI-MS *m/z* (MeOH) ($M-Cl^-$) appropriate isotope pattern, maximum at 718.1 (100%), ($M-Cl^--PPh_3$) appropriate isotope pattern, maximum at 456.2 (41%); Anal. Calcd for $C_{38}H_{37}ClN_2PO_4Ru$: C 60.60, H 4.95, N 3.72. Found: C 60.22, H 4.92, N 3.67.

Na[Ru(III)(3,3'-bismethoxy)salen'$(CN)_2$: (3)

Sodium cyanide (156 mg, 3.19 mmol) and **2** (1.20 g, 1.59 mmol) were refluxed in MeOH (35 mL) for 1 h. The solvent was removed *in vacuo* and the crude material was recrystallized from hot EtOH. This afforded 449 mg (64%) of **3**. Single crystals suitable for diffraction were obtained from hot MeOH. ESI-MS *m/z* (MeOH) ($M-Na^+$) Ru isotope pattern, maximum at 504.8 (100%); Anal. Calcd for $C_{22}H_{22}N_4NaO_4Ru \bullet 1.5H_2O$: C 47.40, H 4.52, N 10.05. Found: C 47.36, H 4.21, N 9.85.

Ru(III)-Ru(III) dimer: (4)

To a partial solution of **3** (35.2 mg, 0.066 mmol) in acetonitrile (5 mL) was added a solution of $Gd(NO_3)_3 \bullet 6(H_2O)$ (33 mg, 0.073 mmol) in acetonitrile (3 mL) resulting in a blue solid that was collected by vacuum filtration. The solid was washed with acetonitrile and diethyl ether. The crystal used for the X-ray diffraction study of **4** was obtained from layering diethyl ether onto a methanolic solution of the crude blue solid after two months.

[Ru(III)(3,3'-bismethoxy)salen'(PPh_3)(H_2O)]$_2$[Gd(III)(NO_3)$_5$]: (5)

To a solution of **2** (132 mg, 0.175 mmol) in acetone (5 mL) was added a solution of $Gd(NO_3)_3$•6(H_2O) (95 mg, 0.210 mmol) in acetone (3 mL). The mixture was refluxed for 45 min and allowed to stir for an additional 2 h at room temperature. A red-brown microcrystalline solid formed upon storage at -20 °C. The solid was isolated by filtration, washed with Et_2O and dried under vacuum yielding 100 mg (57%) of compound **5**. X-ray quality crystals were obtained by slow vapor diffusion of Et_2O into a solution of **5** in acetonitrile at 4 °C. Anal. Calcd for $C_{78}H_{78}N_9O_{25}P_2Ru_2Gd$: C 47.08, H 4.06, N 6.50. Found: C 47.30, H 3.91, N 6.12.

Methyl salicylate:

Salicylic acid (20 g, 144.8 mmol) was dissolved in MeOH (200 mL) and 12 mL of concentrated H_2SO_4 were added over 5 min. The solution was refluxed for 15 h, cooled and quenched with solid $NaHCO_3$ until basic by pH paper. The reaction mixture was concentrated and ethyl acetate and water (200 mL each) were added. The layers were separated and the organic portion was washed with water, saturated aqueous $NaHCO_3$ and brine. The solution was dried over $MgSO_4$, filtered and the solvent was removed *in vacuo*, yielding 19.8 g (90%) of the wintergreen scented methyl salicylate. ^{1}H NMR (500 MHz, DMSO-d_6): δ 3.89 (s, 3H), 6.94 (t, 1H, J = 8 Hz) 6.98 (d, 1H, J = 8 Hz), 7.52 (t, 1H, J = 8 Hz), 7.78 (d, 1H, J = 8 Hz), 10.52 (s, 1H); ^{13}C NMR (126 MHz, DMSO-d_6) δ 52.5, 113.0, 117.4, 119.4, 130.0, 135.7, 160.0, 169.3.

3-Formyl methyl salicylate:

To methyl salicylate (3.01 g, 19.78 mmol) in an oven-dried Schlenk flask under N_2 was added dry methylene chloride (25 mL). The clear, colorless solution was cooled

to 0 °C and $TiCl_4$ (4.4 mL, 39.6 mmol) was added dropwise over 15 min generating a rust colored suspension. Cl_2CHOMe (2.11 mL, 23.7 mmol) was then added over 12 min. The solution was allowed to stir for 48 h and then quenched by pouring into ice water (30 mL). The resulting emulsion was separated and the aqueous layer washed 2 x with methylene chloride (35 mL). The combined organics were washed with water and brine, dried over $MgSO_4$ and concentrated. The crude product was purified by chromatography (silica, 10% EtOAc in hexanes) to yield 400 mg (11%) of product. ^{1}H NMR (500 MHz, $CDCl_3$): δ 4.00 (s, 3H), 7.00 (t, 1H, *J* = 7.5 Hz) 8.02 (dd, 1H, *J* = 7.5 Hz, *J'* = 1.5 Hz), 8.10 (dd, 1H, *J* = 7.5 Hz, *J'* = 1.5 Hz), 10.50 (s, 1H), 11.54 (s, 1H).

(3,3'-bismethoxycarbonyl)salen: (6)

3-formyl methyl salicylate (100 mg, 0.555 mmol) was dissolved in EtOH (5 mL). Ethylenediamine (18.6 μL, 0.278 mmol) was added via micropipette resulting in a yellow precipitate. The solid was collected on filter paper and washed with a minimal amount of EtOH, followed by Et_2O and dried *in vacuo*. This yielded 88 mg (82%) of compound **6**.

4-Methyl methyl salicylate:

4-methyl salicylic acid (15 g, 98.6 mmol) was dissolved in MeOH (150 mL) and 10 mL of concentrated H_2SO_4 were added over 5 min. The solution was refluxed for 16 h, cooled and quenched with solid $NaHCO_3$ until basic by pH paper. The reaction mixture was concentrated and ethyl acetate and water (200 mL each) were added. The layers were separated and the organic portion washed with water, saturated aqueous $NaHCO_3$ and brine. The solution was dried over $MgSO_4$, filtered and the solvent removed *in vacuo*, yielding 15.4 g (94%) of the licorice scented 4-methyl methyl salicylate.

3-Formyl-4-methyl methyl salicylate:

To 4-methyl methyl salicylate (4.17 g, 25.1 mmol) in an oven-dried Schlenk flask under N_2 was added dry methylene chloride (40 mL). The clear, pale brown solution was cooled to 0 °C and $TiCl_4$ (5.5 mL, 50.2 mmol) was added dropwise over 5 min generating a rust colored suspension. To facilitate stirring, dry methylene chloride (5 mL) was added. Cl_2CHOMe (2.67 mL, 30.1 mmol) was then added over 5 min. The solution was allowed to stir for 72 h and then quenched by pouring into ice water (150 mL). The resulting emulsion was separated and the aqueous layer was washed 3 x with methylene chloride (50 mL). The combined organics were washed with water and brine, dried over $MgSO_4$ and concentrated. The crude product was dissolved in hot diethyl ether (100 mL), filtered hot and concentrated to 50 mL. The white crystalline product was collected yielding 1.39 g (29%) of the desired compound. An additional 410 mg of product was obtained upon purification of the supernatant by chromatography (silica, 10% EtOAc in hexanes) to yield a total of 1.80 g (37%) of product.

(3,3'-bismethoxycarbonyl-4,4'-dimethyl)salen: (7)

3-Formyl-4-methyl methyl salicylate (410 mg, 2.12 mmol) was dissolved in 7 mL EtOH. Ethylenediamine (70.7 μL, 1.06 mmol) was added via micropipette resulting in a hazy yellow suspension. Diethyl ether (30 mL) was added and the suspension was cooled at -20 °C. The resulting solid was collected on filter paper and washed with a minimal amount of Et_2O and dried *in vacuo*. This yielded 193 mg (44%) of compound **7**. ^{1}H NMR (500 MHz, $CDCl_3$): δ 2.41 (s, 6H), 3.90 (s, 6H), 3.98 (s, 4H), 6.62 (d, 2H, J = 8 Hz) 7.81 (d, 2H, J = 8 Hz), 8.65 (s, 2H) ; ^{13}C NMR (126 MHz, $CDCl_3$) δ 19.7, 52.4, 59.2, 117.5, 120.5, 136.1, 145.3, 164.1, 164.8, 216.1.

2-Bromo-6-methyl phenol: (10)[34]

To a solution of 2-methyl phenol (5.0 g, 46.2 mmol) in methylene chloride (90 mL) was added diisopropylamine (655 μL, 4.62 mmol) in methylene chloride (23 mL). To the resulting clear colorless solution was added *N*-bromosuccinimide (8.25 g, 46.2 mmol) in methylene chloride (240 mL) over the course of 1 h. The solution was allowed to stir for 1 h at which point the reaction was quenched with 0.1N H_2SO_4 (350 mL). The layers were separated and the organic portion was dried over $MgSO_4$, filtered and concentrated *in vacuo*. The crude was purified by column chromatography (silica, hexanes) to yield 7.32 g (85%) product. ^{1}H NMR (400 MHz, $CDCl_3$): δ 2.29 (s, 3H), 5.54 (s, 1H), 6.71 (m, 1H) 7.06 (d, 1H, J = 7.6 Hz), 7.29 (d, 1H, J = 8.8 Hz).

1-Bromo-2-methoxy-3-methyl benzene: (9)

To a suspension of potassium carbonate (3.6 g, 26.0 mmol) and bromo phenol **10** (2.43 g, 13.0 mmol) in methylethylketone (30 mL) was added dimethylsulfate (2.5 mL, 26.0 mmol) via syringe. The mixture was refluxed for 1.25 h, cooled and quenched with 1 N HCl (70 mL). Diethyl ether (50 mL) was added and the layers separated. The aqueous layer was washed with diethyl ether (50 mL) and the combined organics were dried over $MgSO_4$ and concentrated *in vacuo*. The crude was dissolved in hexanes and run through a plug of silica to yield 2.32 g (89%) of product, **9**. The product was pure by TLC (silica, hexanes).

2,9-Bis-(2-methoxy-3-methyl-phenyl)-[1,10]phenanthroline: (8)

After washing oil-coated Li metal (123 mg, ~16 mmol) with dry diethyl ether, the metal was suspended in dry diethyl ether (5 mL). Compound **9** (1.60 g, 7.96 mmol) was dissolved in dry diethyl ether (5 mL) and transferred via cannula to the metal suspension.

The mixture was refluxed until all lithium dissolved (1.5 h) and the resulting solution was transferred via cannula to a 0 °C solution of dry 1,10-phenanthroline (359 mg, 1.99 mmol, dried for 2 h at 80 °C under vacuum) dissolved in dry THF (5 mL). The solution was allowed to warm to room temperature and checked periodically by mass spectroscopy. After 4 days, degassed water was added to quench the reaction. Methylene chloride (30 mL) was added and the layers were separated. The aqueous portion was washed with methylene chloride, the organics were then pooled, dried over $MgSO_4$, filtered and concentrated *in vacuo*. The crude material was dissolved in acetone (35 mL) and cooled to 0 °C. A saturated solution of $KMnO_4$ in acetone was added dropwise to this solution until a purple color persisted, at which time isopropanol was added. The suspension was filtered through Celite and concentrated. The crude material was purified by column chromatography (silica 20% EtOAc in hexanes, $R_f = 0.30$) to yield 80 mg (9.6%) of compound **8**. ^{1}H NMR (500 MHz, $CDCl_3$): δ 2.39 (s, 6H), 3.63 (s, 6H) 7.21 (m, 2H), 7.27 (d, 2H, $J = 7$ Hz), 7.79 (s, 2H), 8.02 (d, 2H, $J = 7.5$ Hz), 8.26 (m, 4H); ^{13}C NMR (125 MHz, $CDCl_3$) δ 16.4, 61.3, 124.4, 124.5, 126.2, 127.7, 130.4, 131.6, 132.2, 134.2, 136.1, 146.4, 156.9, 157.0; ESI-MS *m/z* (MeOH) ($M+H^+$) 421.1 (100%), ($M+Na^+$) 443.1 (28%).

X-ray Crystallography:

The crystallographic data were collected and solved by Dr. Charlotte Stern of the Analytical Services Laboratory at Northwestern University. The data were collected on a Bruker SMART 1000 X-ray diffractometer with CCD detector using graphite monochromated Mo Kα radiation (λ = 0.71073 Å). Data sets for **2**, **3** and **4** were obtained at 153(2) K while data was collected for **5** at 293(2) K. For **2** the data were

collected with a theta range of 1.96 to 28.95º. Data were obtained in 0.3º oscillations with 10 s exposures. For **3**, the theta range for data collection was 1.70 to 28.97º and data were collected in 0.3º oscillations with 25 s exposures. For **4**, the theta range was 1.12 to 29.04º and data were collected in 0.3º oscillations with 30 s exposures. The crystal-to-detector distance was 50.00 mm with the detector at the 28º swing position for all structures. Data were processed using SAINT-NT from Bruker and were corrected for Lorentz and polarization effects. The structures were solved by direct methods,[35] expanded using Fourier techniques and refined by full matrix least squares on F^2.[36] The non-hydrogen atoms were refined anisotropically. Hydrogen atoms were included in idealized positions but not refined with the exception of the hydroxyl hydrogen in the methanol solvates of **3**. Compound **4** showed half occupancy of Na atoms, and the H-atoms on the water and methanol hydroxyl were not included. These H-atoms could not be located in reasonable positions. H-atoms for compound **5** were not included in the refinement. Crystallographic data for **2** and **3** are tabulated in Table 3-2 with selected bond lengths and angles given in Table 3-3. Crystallographic data for **4** and **5** are collected in Table 3-4.

References

[1] Caravan, P., Ellison, J.J., McMurry, T.J., Lauffer, R.B. (1999) Gadolinium(III) chelates as MRI contrast agents: Structure, dynamics, and applications. *Chemical Reviews,* **99**: 2293-2352.

[2] Woods, M., Botta, M., Avedano, S., Wang, J., Sherry, A.D. (2005) Towards the rational design of MRI contrast agents: A practical approach to the synthesis of gadolinium complexes that exhibit optimal water exchange. *Dalton Transactions*: 3829-3837.

[3] Clementi, V., Luchinat, C. (1998) NMR and spin relaxation in dimers. *Accounts of Chemical Research,* **31**: 351-361.

[4] Banci, L., Bertini, I., Luchinat, C.: Nuclear and electron relaxation: The magnetic nucleus-unpaired electron coupling in solution. VCH, Weinheim; New York 1991.

[5] Costes, J.P., Dahan, F., Dupuis, A., Laurent, J.P. (1997) A general route to strictly dinuclear Cu(II)/Ln(III) complexes. Structural determination and magnetic behavior of two Cu(II)/Gd(III) complexes. *Inorganic Chemistry,* **36**: 3429-3433.

[6] Costes, J.-P., Dahan, F., Dupuis, A. (2000) Influence of anionic ligands (X) on the nature and magnetic properties of dinuclear $LCuGdX_3 \cdot nH_2O$ Complexes (LH_2 standing for tetradentate Schiff base ligands deriving from 2-hydroxy-3-methoxybenzaldehyde and X being Cl, N_3C_2, and CF_3COO). *Inorganic Chemistry,* **39**: 165-168.

[7] Costes, J.-P., Dahan, F., Dupuis, A., Laurent, J.-P. (1996) A genuine example of a discrete bimetallic (Cu, Gd) complex: Structural determination and magnetic properties. *Inorganic Chemistry,* **35**: 2400-2402.

[8] Costes, J.-P., Dahan, F., Dupuis, A., Laurent, J.-P. (2000) Is ferromagnetism an intrinsic property of the Cu(II)/Gd(III) couple? 1. Structures and magnetic properties of two novel dinuclear complexes with a -μ-phenolato-μ-oximato (Cu,Gd) core. *Inorganic Chemistry,* **39**: 169-173.

[9] Costes, J.-P., Dahan, F., Dupuis, A., Laurent, J.-P. (1998) Structural studies of a dinuclear (Cu, Gd) and two trinuclear (Cu_2, Ln) complexes (Ln = Ce, Er). Magnetic properties of two original (Cu, Gd) complexes. *New Journal of Chemistry,* **22**: 1525-1529.

[10] Ramade, I., Kahn, O., Jeannin, Y., Robert, F. (1997) Design and magnetic properties of a magnetically isolated Gd(III)Cu(II) pair. Crystal structures of $[Gd(hfa)_3Cu(salen)]$, $[Y(hfa)_3Cu(salen)]$, $[Gd(hfa)_3Cu(salen)(Meim)]$, and $[La(hfa)_3(H2O)Cu(salen)]$ (hfa = hexafluoroacetylacetonato, salen = N,N'-ethylenebis(salicylideneaminato), Meim = 1-methylimidazole). *Inorganic Chemistry,* **36**: 930-936.

[11] Leung, W.H., Che, C.M. (1989) Oxidation chemistry of ruthenium-salen complexes. *Inorganic Chemistry,* **28**: 4619-4622.

[12] Khan, M.M.T., Mirza, S.A., Rao, A.P., Sreelatha, C. (1988) Synthesis, oxygenation and catalytic properties of ruthenium(III) SALOPH complexes. *Journal of Molecular Catalysis,* **44**: 107-115.

[13] Khan, M.M.T., Shaikh, Z.A., Kureshy, R.I., Boricha, A.B. (1992) Synthesis, characterization and reversible binding of dioxygen and carbon monoxide in ruthenium(III) Schiff base complexes. Effect of equatorial substitution on the dioxygen and carbon monoxide affinities. *Polyhedron,* **11**: 91-100.

[14] Khan, M.M.T., Sreelatha, C., Mirza, S.A., Ramachandraiah, G., Abdi, S.H.R. (1988) Synthesis and characterization of some ruthenium(V) oxo complexes of the Schiff base, bis(salicylidene)-o-phenylenediamine, with appended Cl^-, imidazole and 2-methylimidazole: the first examples of stable oxo complexes via direct oxygenation. *Inorganica Chimica Acta,* **154**: 103-108.

[15] Mihara, J., Hamada, T., Takeda, T., Irie, R., Katsuki, T. (1999) Photo-controlled Lewis acidity. Chiral (ON)Ru-salen-catalyzed hetero Diels-Alder reaction and kinetic resolution of racemic epoxides. *Synlett*: 1160-1162.

[16] Takeda, T., Irie, R., Shinoda, Y., Katsuki, T. (1999) Ru-salen catalyzed asymmetric epoxidation. Photoactivation of catalytic activity. *Synlett*: 1157-1159.

[17] Uchida, T., Irie, R., Katsuki, T. (1999) Chiral (ON)Ru-salen-catalyzed cyclopropanation. High cis- and enantioselectivity. *Synlett*: 1163-1165.

[18] Odenkirk, W., Rheingold, A.L., Bosnich, B. (1992) Homogeneous catalysis: A ruthenium-based Lewis-acid catalyst for the Diels-Alder reaction. *Journal of the American Chemical Society,* **114**: 6392-6398.

[19] Works, C.F., Ford, P.C. (2000) Photoreactivity of the ruthenium nitrosyl complex, Ru(salen)(Cl)(NO). Solvent effects on the back reaction of NO with the Lewis acid Ru(III)(salen)(Cl). *Journal of the American Chemical Society,* **122**: 7592-7593.

[20] Murray, K.S., Van den Bergen, A.M., West, B.O. (1978) Ruthenium complex with a tetradentate salicylaldimine Schiff base. *Australian Journal of Chemistry,* **31**: 203-207.

[21] Aratake, Y., Okawa, H., Asato, E., Sakiyama, H., Kodera, M., Kida, S., Sakamoto, M. (1990) Cobalt(II)-lanthanoid(III) (Ln = La, Nd, or Gd) complexes of N,N'-ethylenebis(3-carboxysalicylideneimine). Interaction of ligating groups on the Co-Ln center. *Journal of the Chemical Society, Dalton Transactions: Inorganic Chemistry (1972-1999)*: 2941-2945.

[22] Matsumoto, N., Sakamoto, M., Tamaki, H., Okawa, H., Kida, S. (1990) Ferromagnetic spin-coupling in a binuclear copper(II)-gadolinium(III) complex. *Chemistry Letters*: 853-854.

[23] Sakamoto, M., Ohsaki, M., Yamamoto, K., Nakayama, Y., Matsumoto, A., Okawa, H. (1992) Synthesis, characterization, and properties of V(IV)O-Ln(III)

(Ln = La, Pr, Eu, Gd, Tb) complexes of N,N'-bis(3-carboxysalicylidene)ethylenediamine. *Bulletin of the Chemical Society of Japan,* **65**: 2514-2519.

[24] Sakamoto, M., Hashimura, M., Nakayama, Y., Matsumoto, A., Okawa, H. (1992) Fluorescence quenching of europium(III) by heteronuclear complex formation with copper(II) or nickel(II). *Bulletin of the Chemical Society of Japan,* **65**: 1162-1164.

[25] Sakamoto, M., Ishimori, T., Okawa, H. (1988) Specific binding of substrates containing nitrogen and oxygen donor groups to copper(II)-gadolinium(III) hetero-metal center. *Bulletin of the Chemical Society of Japan,* **61**: 3319-3320.

[26] Sakamoto, M., Takagi, M., Ishimori, T., Okawa, H. (1988) Copper(II)-lanthanoid(III) complexes of binucleating ligands derived from 3-formylsalicylic acid and diamines. *Bulletin of the Chemical Society of Japan,* **61**: 1613-1618.

[27] Duff, J.C., Bills, E.J. (1934) Reactions between hexamethylenetetramine and phenolic compounds. II. Formation of phenolic aldehydes. Distinctive behavior of p-nitrophenol. *Journal of the Chemical Society, Abstracts*: 1305-1308.

[28] Duff, J.C., Bills, E.J. (1932) Reactions between hexamethylenetetramine and phenolic compounds. I. A new method for the preparation of 3- and 5-aldehydosalicylic acids. *Journal of the Chemical Society, Abstracts*: 1987.

[29] Larrow, J.F., Jacobsen, E.N., Gao, Y., Hong, Y., Nie, X., Zepp, C.M. (1994) A practical method for the large-scale preparation of [N,N'-Bis(3,5-di-tertbutylsalicylidene)-1,2-cyclohexanediaminato(2-)]manganese(III) chloride, a highly enantioselective epoxidation catalyst. *Journal of Organic Chemistry,* **59**: 1939-1942.

[30] Eliel, E.L., Rivard, D.E. (1952) Photobromination of substituted toluenes as a route to substituted benzyl alcohols and benzaldehydes. *Journal of Organic Chemistry,* **17**: 1252-1256.

[31] Jones, G.B., Moody, C.J. (1989) Structurally modified antitumor agents. Part 2. Total synthesis of a cyclopropamitosene. *Journal of the Chemical Society, Perkin Transactions 1: Organic and Bio-Organic Chemistry (1972-1999)*: 2455-2462.

[32] Evans, I.P., Spencer, A., Wilkinson, G. (1973) Dichlorotetrakis(dimethyl sulfoxide)ruthenium(II) and its use as a source material for new ruthenium(II) complexes. *Journal of the Chemical Society, Dalton Transactions: Inorganic Chemistry (1972-1999)*: 204-209.

[33] Lam, F., Feng, M., Chan, K.S. (1999) Synthesis of dinucleating phenanthroline-based ligands. *Tetrahedron,* **55**: 8377-8384.

[34] Fujisaki, S., Eguchi, H., Omura, A., Okamoto, A., Nishida, A. (1993) Halogenation using N-halo compounds. I. Effect of amines on ortho-bromination of phenols with NBS. *Bulletin of the Chemical Society of Japan,* **66**: 1576-1579.

[35] Sheldrick, G.M. (1997): SHELXS-97, Program for Crystal Structure Determination. University of Göttingen, Germany.

[36] Sheldrick, G.M. (1997): SHELXL-97, Program for the Refinement of Crystal Structures. University of Göttingen, Germany.